Table S1: Summary of selected prior work characterizing size-resolved organic acids and methanesulfonate (MSA).

Location	Selected Species	Reference
Arctic		
Arctic	MSA, oxalate, succinate	Kerminen et al. (1999)
Asia		
Chengdu, China	Oxalate, succinate, adipate, maleate, phthalate	Cheng et al. (2015) Huang et al. (2019)
Shanghai, China	MSA, oxalate	Ding et al. (2017)
North, west, and south of Japan	Oxalate, succinate	Gao et al. (2003)
Gwangju, Korea	Oxalate	Park and Kim (2014)
Baoji, China Mt. Tai, China Okinawa Island, Japan	Succinate, phthalate	Wang et al. (2017)
Xi'an, China	Oxalate, succinate, adipate, maleate, phthalate	Wang et al. (2012)
Hong Kong	Oxalate, succinate	Yao et al. (2002)
Europe		
Finokalia, Greece	MSA, oxalate, succinate	Bardouki et al. (2003)
Sagres, Portugal Melpitz, Germany	MSA, oxalate, succinate, adipate	Neusüss et al. (2000)
Melpitz, Germany Falkenberg, Germany Goldlauter, Germany Leipzig, Germany Dresden, Germany	Oxalate, succinate	van Pinxteren et al. (2014)
Po Valley, Italy	Oxalate	Sandrini et al. (2016)
North America		
Central California	MSA, succinate, maleate, oxalate	Maudlin et al. (2015)
California	Oxalate	Murphy et al. (2009)
Hayden and Winkelman, Arizona	Oxalate	Sorooshian et al. (2012)
Thompson Farm and Shoals, New England	Oxalate, succinate, maleate, MSA	Ziemba et al. (2011)
South America		
Rondônia, Brazil	MSA, oxalate, succinate, maleate, adipate, phthalate	Blazso et al. (2003) Decesari et al. (2006) Falkovich et al. (2005)
Other		
North Pacific East Asia	Oxalate, succinate	Mochida et al. (2003)
Tudor Hill, Bermuda	Oxalate	Turekian et al. (2003)

Table S2: MOUDI sample set details including sample start date and time, sampling flow rate, sample duration, and average values of both the temperature of the MOUDI housing and relative humidity (RH) of ambient air. Sets marked with "*" are sets with gravimetric data.

Sample ID	Start Date (Local)	Flow (L min^{-1})	Run Time (h)	Temp. (°C)	RH (%)	Sample ID	Start Date (Local)	Flow (L min^{-1})	Run Time (h)	Temp. (°C)	RH (%)
MO1	07/19/18 12:40	29.6	24	30.5	59.0	**MO31***	02/13/19 15:33	29.9	49	35.8	65.7
MO2	07/23/18 11:29	29.6	54	31.7	66.8	**MO33**	02/23/19 5:00	29.8	48	34.3	58.1
MO4*	07/25/18 19:16	30.3	119	34.4	69.0	**MO34**	03/04/19 14:05	29.4	48	35.3	57.9
MO5	07/30/18 19:17	28.8	42	33.5	66.7	**MO36***	03/12/19 15:50	29.3	48	39.9	56.8
MO6	08/06/18 14:33	27.1	48	34.6	63.3	**MO37**	03/20/19 15:15	30.0	48	38.8	55.1
MO7	08/14/18 13:59	27.9	48	34.9	78.3	**MO38**	03/30/19 5:00	29.6	48	36.4	54.0
MO8	08/22/18 13:46	29.0	48	35.7	78.2	**MO40***	04/08/19 14:30	29.6	48	41.4	57.6
MO9	09/01/18 5:00	27.5	48	34.9	68.4	**MO41**	04/16/19 14:30	29.1	48	38.7	57.7
MO10	09/10/18 14:42	29.0	48	36.7	65.2	**MO42**	04/24/19 14:30	29.1	48	40.3	53.7
MO11	09/18/18 14:12	27.1	48	35.8	68.3	**MO44***	05/04/19 5:00	28.6	48	37.0	59.8
MO12	09/26/18 13:53	27.5	48	37.0	70.9	**MO45**	05/13/19 14:30	28.7	48	37.3	61.8
MO14*	10/06/18 5:00	26.1	48	32.0	73.1	**MO46**	05/21/19 14:30	28.7	48	39.0	72.2
MO15	10/15/18 14:37	29.7	48	37.3	67.6	**MO47**	05/29/19 14:24	28.9	48	39.3	64.5
MO16	10/23/18 14:18	29.2	48	37.6	67.7	**MO48***	06/08/19 5:00	28.0	48	38.9	62.6
MO17	11/06/18 15:42	30.0	48	36.5	60.6	**MO50**	06/17/19 14:20	28.8	48	39.2	64.4
MO18	11/10/18 5:00	29.5	48	36.7	61.9	**MO51**	06/25/19 14:18	27.8	50	36.2	77.1
MO19	11/19/18 13:55	31.4	48	35.8	61.4	**MO53***	07/03/19 14:43	26.9	48	38.8	60.9
MO20	11/27/18 14:16	30.2	48	34.8	60.8	**MO54**	07/13/19 5:00	28.8	48	36.8	66.4
MO21	12/05/18 13:57	30.5	48	34.8	72.0	**MO55**	07/22/19 14:40	28.8	48	38.0	75.4
MO22	12/15/18 5:00	29.6	48	32.7	78.5	**MO56**	07/30/19 14:37	26.7	48	35.0	76.1
MO23	12/24/18 13:30	26.4	48	29.7	81.8	**MO57***	08/07/19 14:18	27.5	48	33.0	94.1
MO24	12/31/18 14:45	30.2	48	35.8	84.6	**MO59**	08/17/19 5:00	28.2	48	37.8	85.9
MO26	01/01/19 13:30	24.1	48	35.0	77.2	**MO60**	08/26/19 14:31	28.2	48	37.3	92.7
MO27	01/09/19 14:48	23.9	48	36.2	65.3	**MO61**	09/03/19 14:28	29.4	48	36.3	62.1
MO28	01/19/19 5:00	25.0	48	33.1	63.5	**MO62***	09/11/19 14:34	27.8	48	36.5	77.0
MO29	01/28/19 14:17	29.5	48	34.5	63.3	**MO64**	09/21/19 5:00	27.0	48	37.5	67.2
MO30	02/05/19 13:30	29.8	48	34.4	60.7	**MO65***	09/30/19 14:30	27.2	48	38.4	65.3

Table S3: Water-soluble species analyzed with their respective recovery ± standard deviation (SD) and limit of detection (LOD) in aqueous concentration units quantified using ICP-QQQ (elements: Al to V) and IC (ions: adipate to sulfate). LOD units for elements and ions are ppt and ppb, respectively.

Species	Recovery ± SD (%)	LOD
Al	96 ± 7	29.474
As	98 ± 10	7.945
Cd	102 ± 11	4.194
K	93 ± 18	10.48
Ni	97 ± 8	2.837
Pb	99 ± 8	0.503
Ti	101 ± 10	39.046
V	95 ± 9	1.353
Adipate	101 ± 4	22.655
Chloride	103 ± 7	2.144
Maleate	100 ± 3	6.97
MSA	102 ± 6	12.316
Nitrate	106 ± 12	8.917
Oxalate	100 ± 2	12.312
Phthalate	99 ± 2	20.685
Sodium	104 ± 8	43.476
Succinate	98 ± 9	11.046
Sulfate	101 ± 3	11.982

Table S4: Summary of positive matrix factorization (PMF) and error estimation diagnostics.

Factors	5
Q_{Robust}	3075
Q_{True}	4369
$Q_{Rob/Exp}$	0.41
$Q/Q_{Exp} > 6$	-
DISP %dQ	-0.0004
DISP swaps	0
Factors with BS mapping < 100%	1
BS-DISP % cases with swaps	0

Table S5: Percentage that each organic acid and MSA contributes to the total mass for all (0.056 – 18 μm), submicrometer, and supermicrometer size ranges, as well as for each individual stage. These percentages were calculated as the mean based on the 11 simultaneously collected MOUDI sets for gravimetric and chemical analysis. "Unresolved" represents the percent difference between the total mass and the following measured constituents: black carbon (BC), and water-soluble ions (Na^+, NH_4^+, Mg^{2+}, Ca^{2+}, dimethylamine (DMA), trimethylamine (TMA), and diethylamine (DEA), methanesulfonate (MSA), pyruvate, adipate, succinate, maleate, oxalate, phthalate, Cl^-, NO_3^-, and SO_4^{2-}) and elements (Ag, Al, As, Ba, Cd, Co, Cr, Cs, Cu, Fe, Hf, K, Mn, Mo, Nb, Ni, Pb, Rb, Se, Sn, Sr, Ti, Tl, V, Y, Zn, and Zr). Error associated with BC is reported as the standard deviation in measured BC as a function of size. Cells marked with "-" denote values of zero.

Stages	Total	Phthalate	Adipate	Succinate	Maleate	Oxalate	MSA	Unresolved	BC Error
All	0.80%	0.03%	0.03%	0.03%	0.04%	0.64%	0.02%	33.74%	21.72%
< 1 μm	0.78%	0.03%	0.01%	0.04%	0.06%	0.60%	0.03%	17.78%	34.27%
> 1 μm	0.84%	0.04%	0.06%	0.02%	-	0.71%	0.01%	69.10%	3.59%
10 – 18	0.63%	-	0.04%	0.04%	-	0.56%	-	79.43%	26.47%
5.6 – 10	0.70%	-	0.21%	0.02%	-	0.45%	0.02%	76.76%	1.04%
3.2 – 5.6	0.56%	0.03%	0.06%	0.02%	-	0.44%	-	73.36%	2.95%
1.8 – 3.2	0.98%	0.07%	0.04%	0.03%	-	0.84%	-	67.60%	3.48%
1.0 – 1.8	1.01%	0.03%	0.03%	0.01%	0.01%	0.93%	0.01%	63.21%	8.68%
0.56 – 1.0	1.06%	0.03%	0.01%	0.05%	0.13%	0.80%	0.04%	36.58%	15.25%
0.32 – 0.56	0.88%	0.04%	0.01%	0.07%	0.06%	0.65%	0.04%	16.04%	29.51%
0.18 – 0.32	0.55%	0.03%	0.01%	0.01%	0.01%	0.46%	0.03%	2.99%	43.55%
0.10 – 0.18	0.56%	-	0.04%	0.05%	-	0.45%	0.02%	7.97%	85.41%
0.056 – 0.10	0.49%	-	-	0.03%	-	0.46%	-	63.88%	49.91%

Table S6: Pearson's correlation matrix (r values) of water-soluble species across all MOUDI sizes (0.056 – 18 μm). Blank boxes indicate p-values exceeding 0.05 and thus deemed to be statistically insignificant. Similar correlation matrices can be seen for submicrometer and supermicrometer sizes in Table 3. Ad – adipate, Su – succinate, Ma – maleate, Ox – oxalate, Ph – phthalate.

	Al	**Ti**	**K**	**Rb**	**V**	**Ni**	**As**	**Cd**	**Pb**	**Na**	**Cl**	**NO3**	**SO4**	**MSA**	**Ad**	**Su**	**Ma**	**Ox**	**Ph**
Al	1.00																		
Ti	0.49	1.00																	
K	0.57		1.00																
Rb	0.63		0.48	1.00															
V				0.36	1.00														
Ni	0.35	0.34		0.41	0.79	1.00													
As		0.41					1.00												
Cd		0.28			0.67	0.69		1.00											
Pb	0.44	0.33	0.30	0.29	0.32	0.42		0.44	1.00										
Na	0.36	0.38								1.00									
Cl	0.54	0.36	0.41							0.78	1.00								
NO3	0.49		0.44	0.31						0.56	0.49	1.00							
SO4			0.32	0.46	0.44							0.50	1.00						
MSA				0.37						0.42		0.35	0.59	1.00					
Ad															1.00				
Su	0.36			0.67						0.38			0.43	0.67		1.00			
Ma															0.45		1.00		
Ox	0.42			0.71	0.44	0.45						0.31	0.69	0.53		0.76		1.00	
Ph	0.41	0.36		0.48						0.53	0.35	0.31	0.34	0.58	0.43	0.73		0.63	1.00

Table S7: Size distribution peaks for each season and respective concentrations. "All" represents the cumulative dataset.

Species	Peak Bins (μm)					Peak Values ($ng\ m^{-3}$)				
	All	SWM18	Trans	NEM	SWM19	All	SWM18	Trans	NEM	SWM19
Phthalate	0.32-0.56 1.8-3.2	0.32-0.56 3.2-5.6	0.32-0.56 3.2-5.6	0.18-0.32 3.2-5.6	0.56-1.0 1.8-3.2	2.1 1.2	5.7 0.81	9.2 2.9	0.68 1.5	1.4 1.8
Adipate	0.10-0.18 0.32-0.56 5.6-10.0	0.32-0.56 5.6-10.0	0.32-0.56 1.0-1.8 5.6-10.0	0.10-0.18 1.8-3.2 5.6-10.0	0.10-0.18 0.56-1.0 3.2-5.6	1.1 1.0 0.95	1.7 0.93	2.2 1.4 0.86	0.86 0.37 0.75	1.6 1.4 2.3
Succinate	0.32-0.56 1.8-3.2	0.32-0.56 1.8-3.2	0.18-0.32 0.56-1.0 3.2-5.6	0.10-0.18 0.32-0.56 1.8-3.2 5.6-10.0	0.56-1.0 1.8-3.2	3.1 0.69	7.8 1.1	1.5 4.0 0.26	0.52 2.0 0.73 0.26	2.5 0.41
Maleate	0.56-1.0	0.56-1.0	0.56-1.0	0.32-0.56	0.56-1.0	5.1	9.9	1.7	0.94	11
Oxalate	0.32-0.56 1.8-3.2	0.32-0.56 1.8-3.2	0.32-0.56 1.8-3.2	0.32-0.56 1.8-3.2	0.56-1.0 1.8-3.2	32 20	35 26	58 30	31 18	28 18
MSA	0.32-0.56 5.6-10.0	0.32-0.56	0.32-0.56 1.8-3.2	0.32-0.56 5.6-10.0	0.32-0.56 5.6-10.0	2.0 0.043	3.5	2.2 0.15	1.2 0.034	2.3 0.11

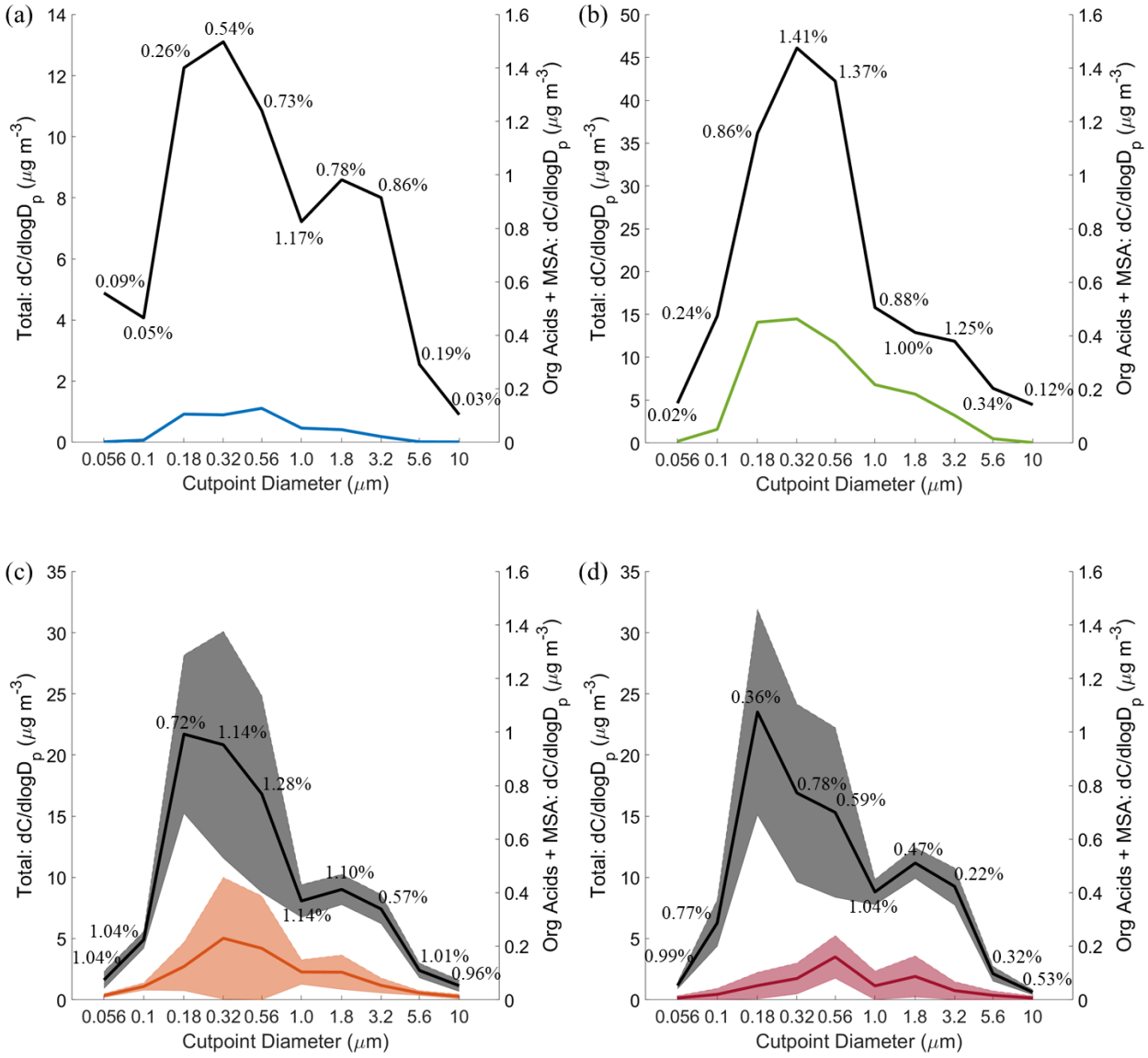

Figure S1: Size-resolved comparison of (black curve) total mass and (colored curve) the sum of measured organic acids and MSA for the (a) 2018 southwest monsoon (SWM18), (b) transitional period (Trans), (c) northeast monsoon (NEM), and (d) 2019 southwest monsoon (SWM19) seasons. Solid lines are the averages and shaded areas represent one standard deviation. The average percent contribution of the organic acids and MSA to total mass is provided for each size bin. These plots are based on data from the 11 MOUDI chemical sets with accompanying gravimetric measurements. It should be noted that SWM18 and Trans each only one gravimetric set and thus standard deviations are unavailable.

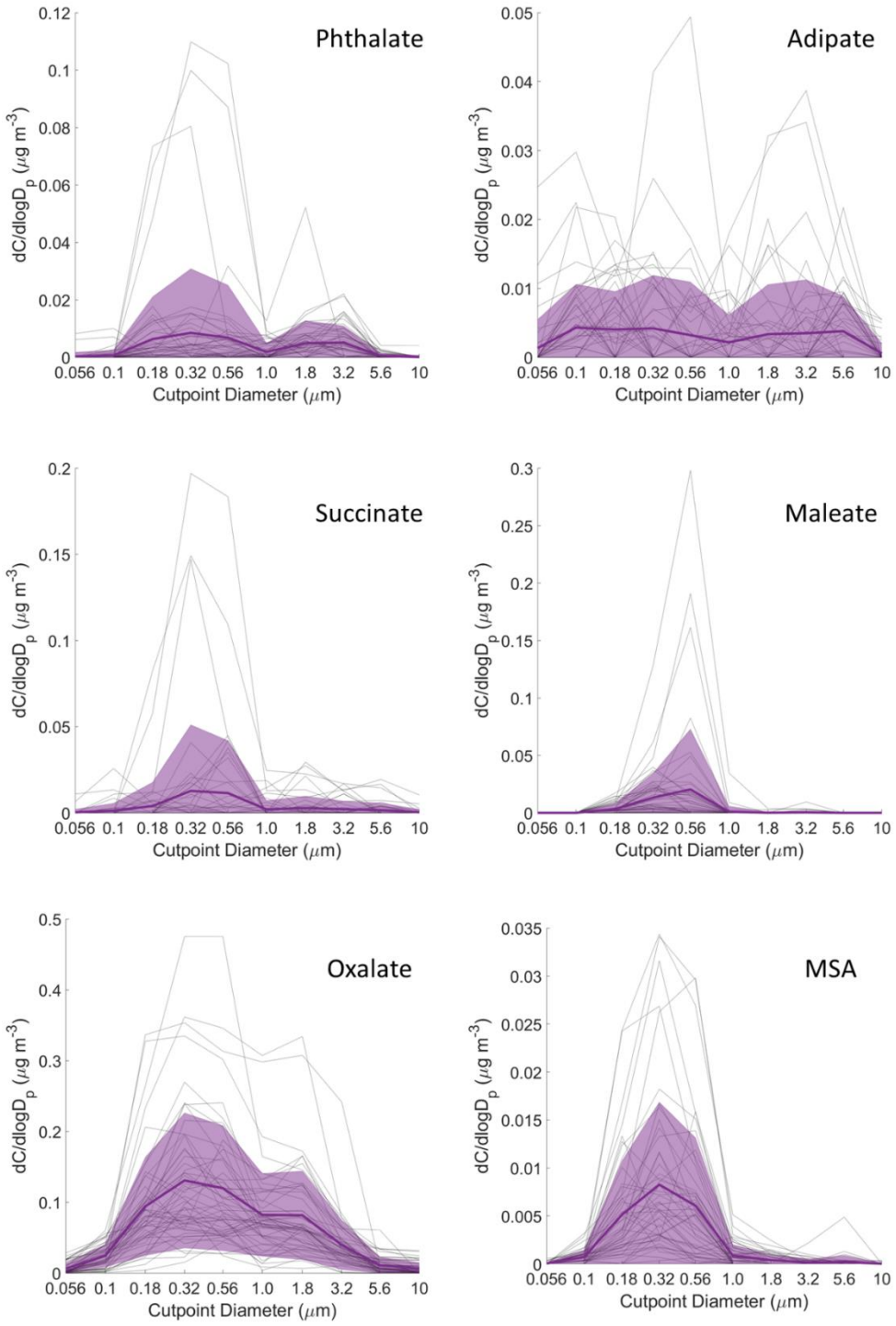

Figure S2: Cumulative size distributions for each organic acid and MSA. The transparent lines are the individual sets, while the thick colored lines and transparent shaded areas represent the mean and standard deviation, respectively, of the cumulative sets.

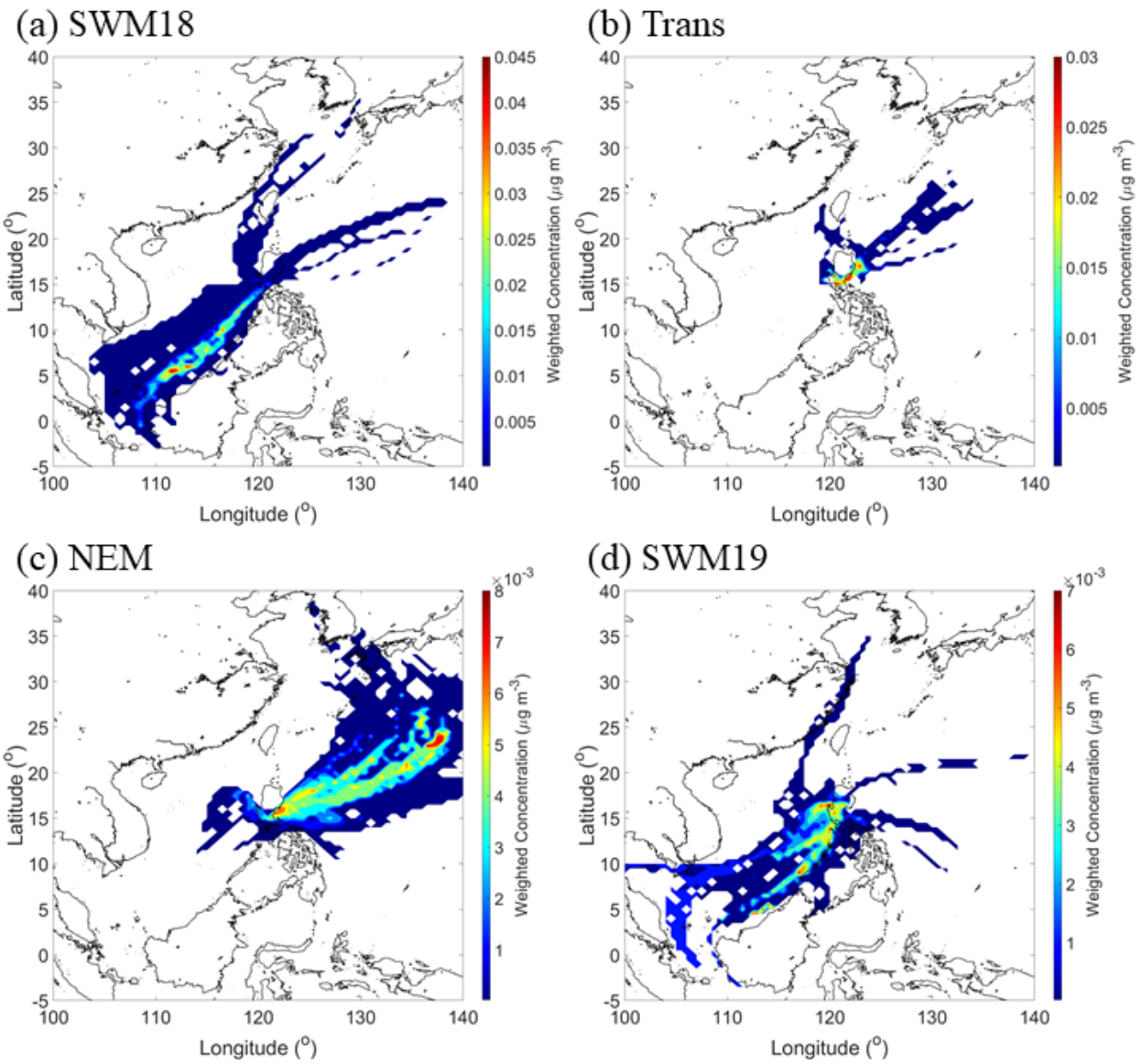

Figure S3: WCWT maps of phthalate for (a) 2018 southwest monsoon (SWM18), (b) transitional period (Trans), (c) northeast monsoon (NEM), and (d) 2019 southwest monsoon (SWM19) for all sizes.

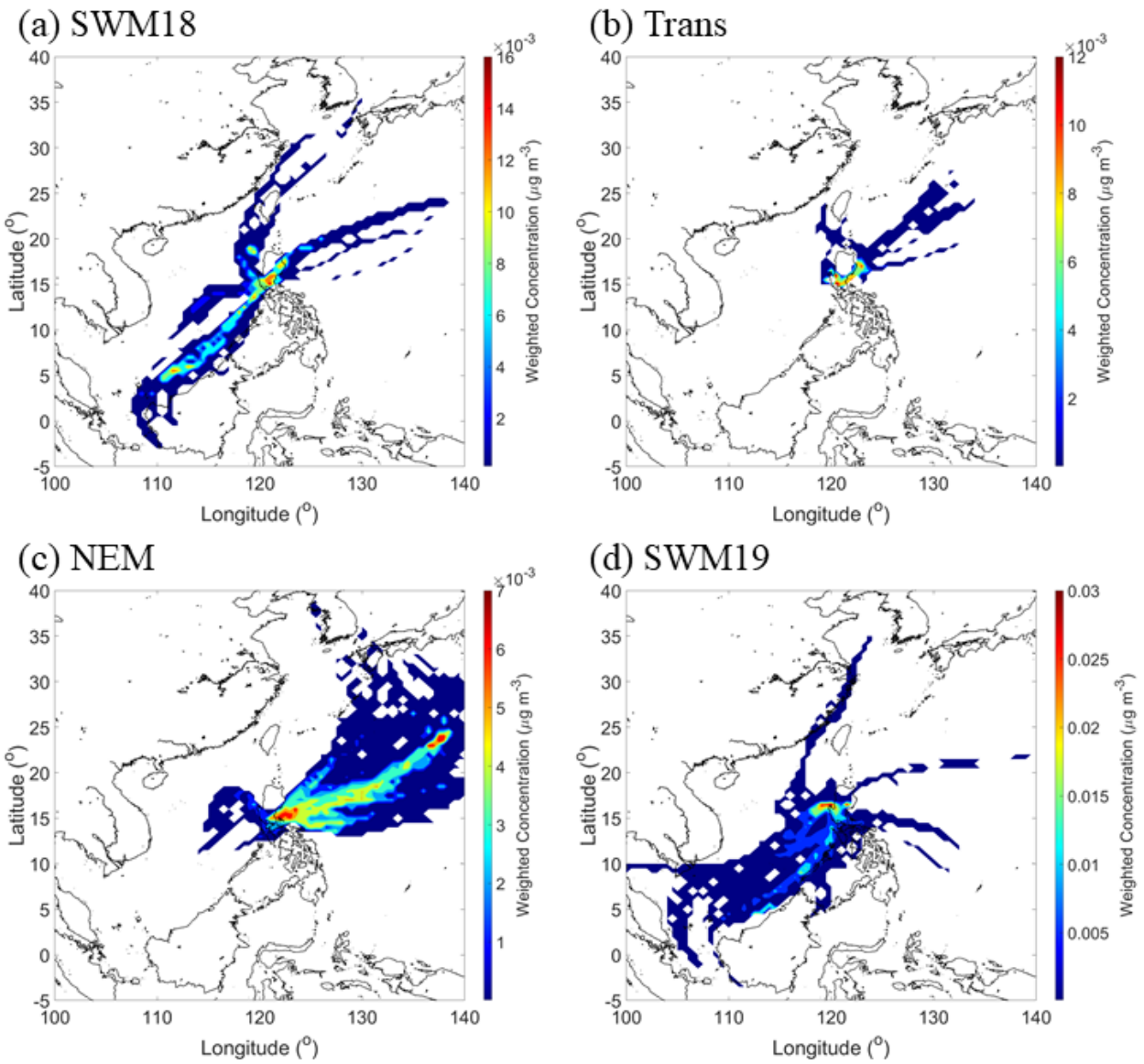

Figure S4: Same as Figure S3 except for adipate.

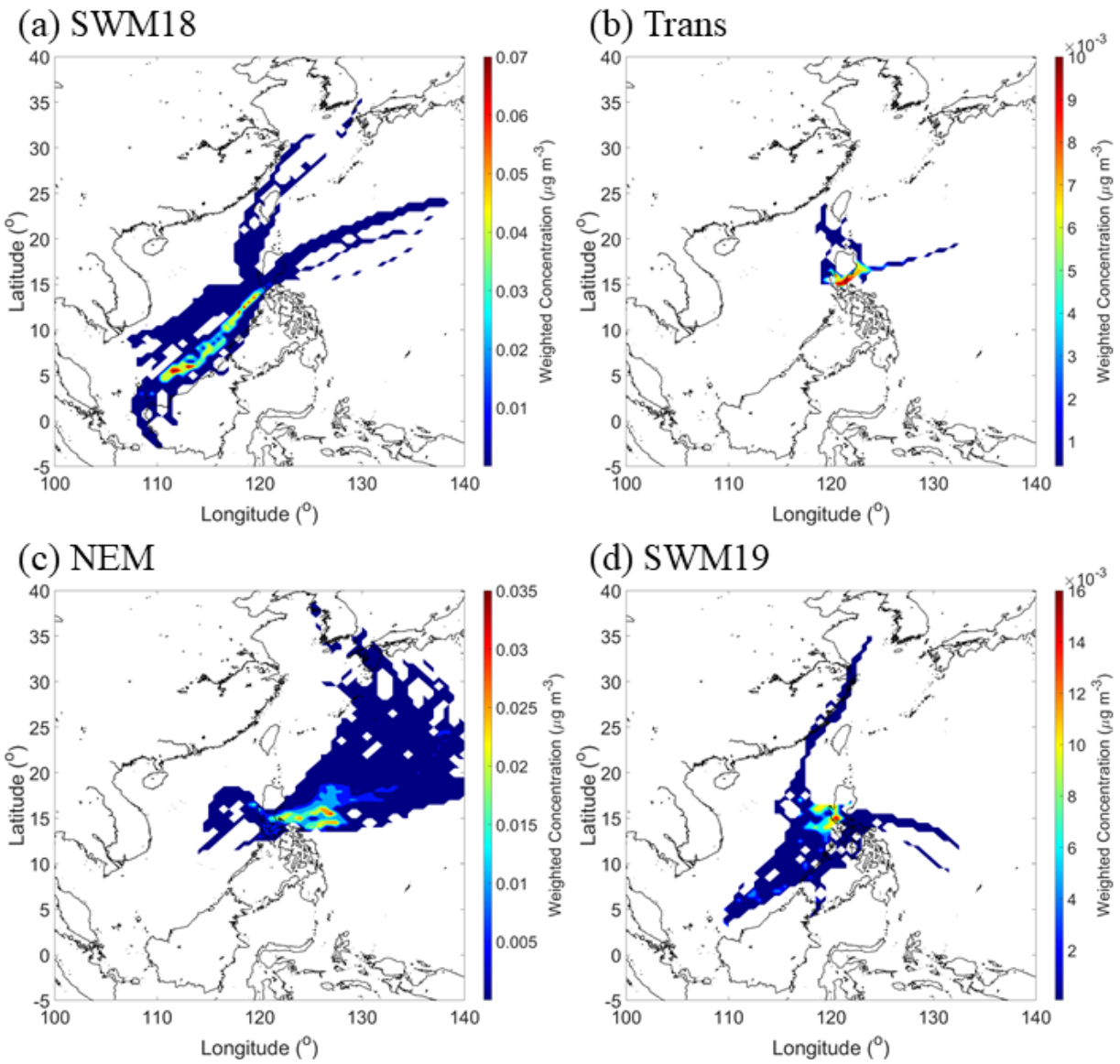

Figure S5: Same as Figure S3 except for succinate.

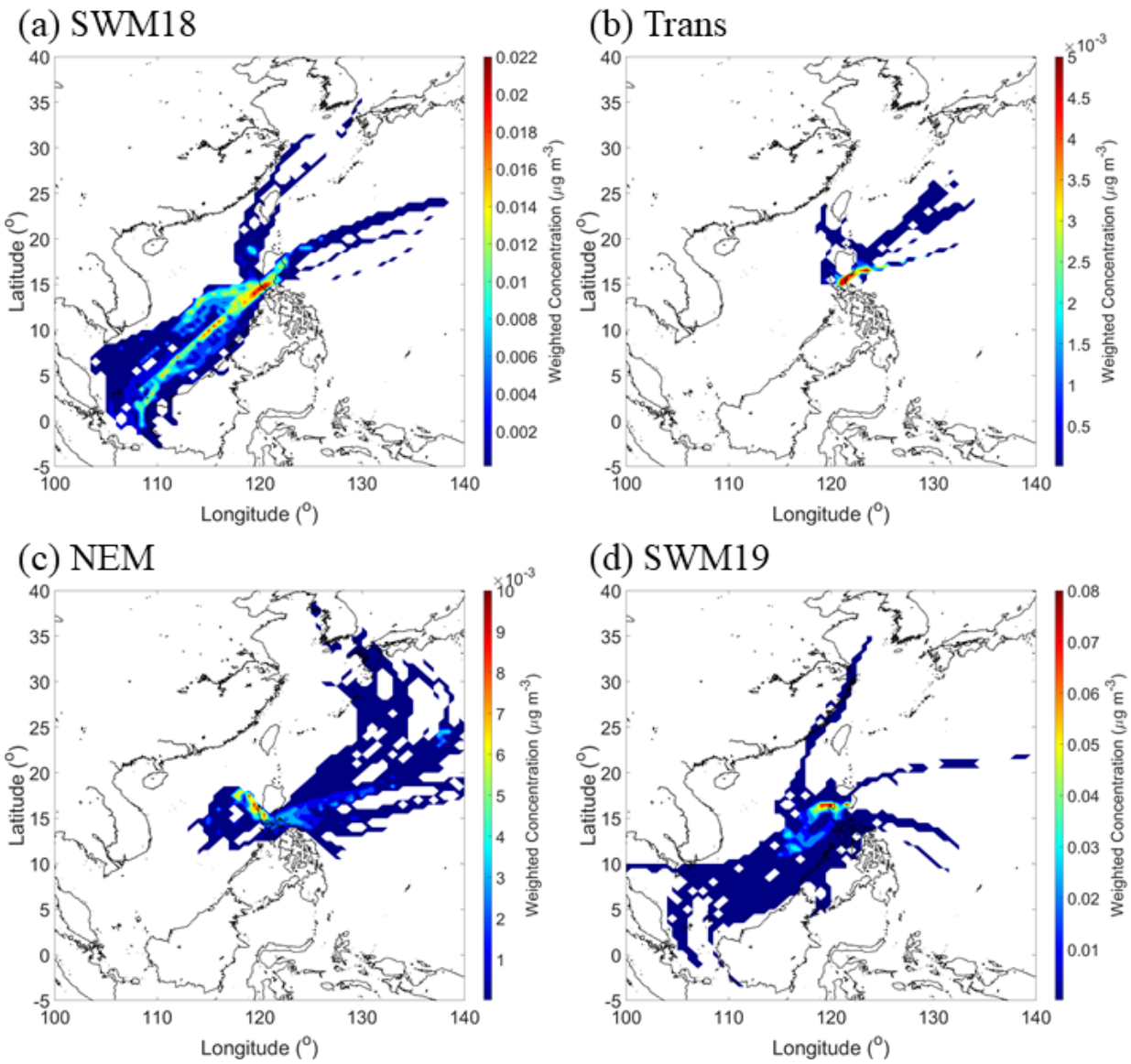

Figure S6: Same as Figure S3 except for maleate.

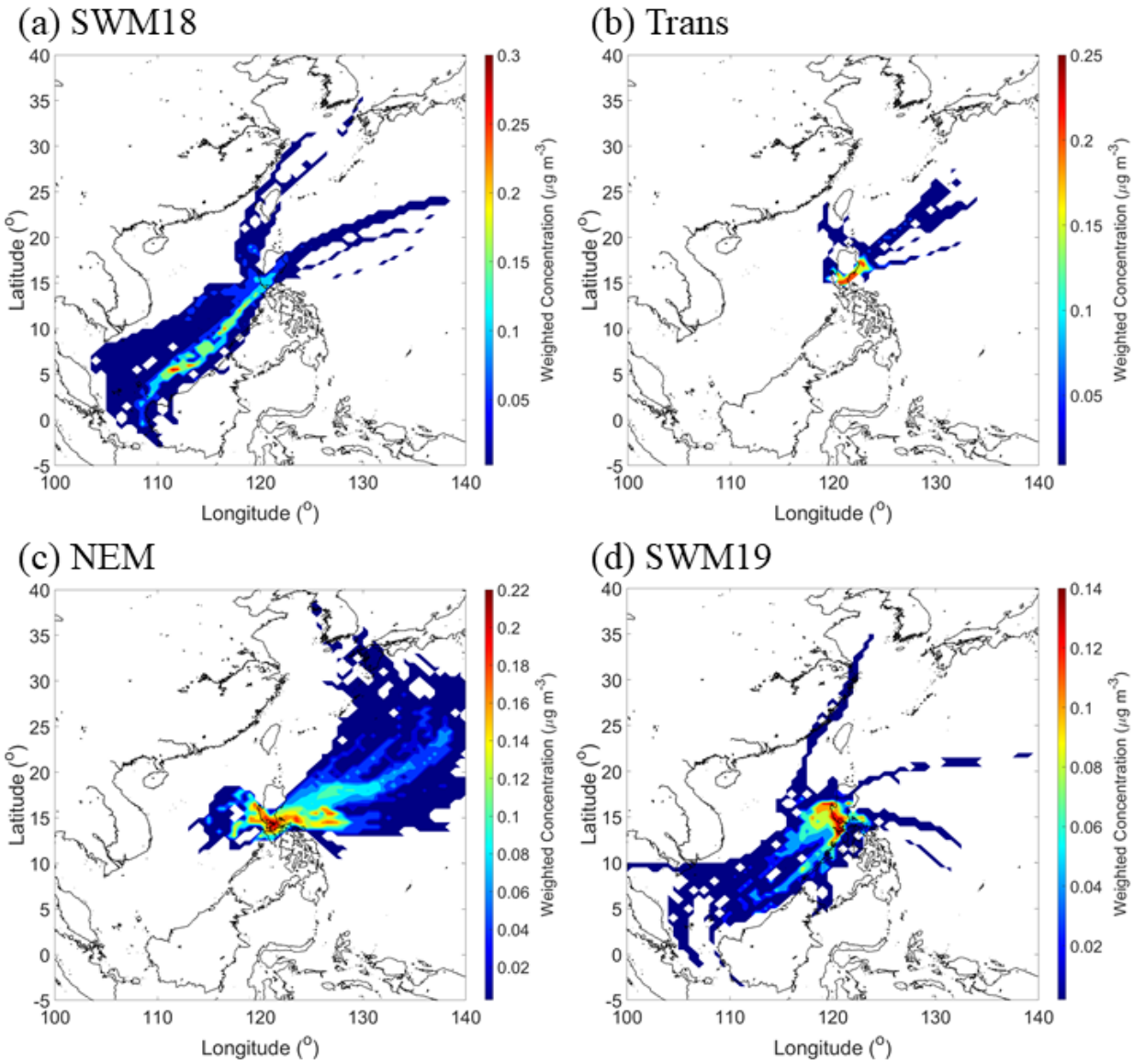

Figure S7: Same as Figure S3 except for oxalate.

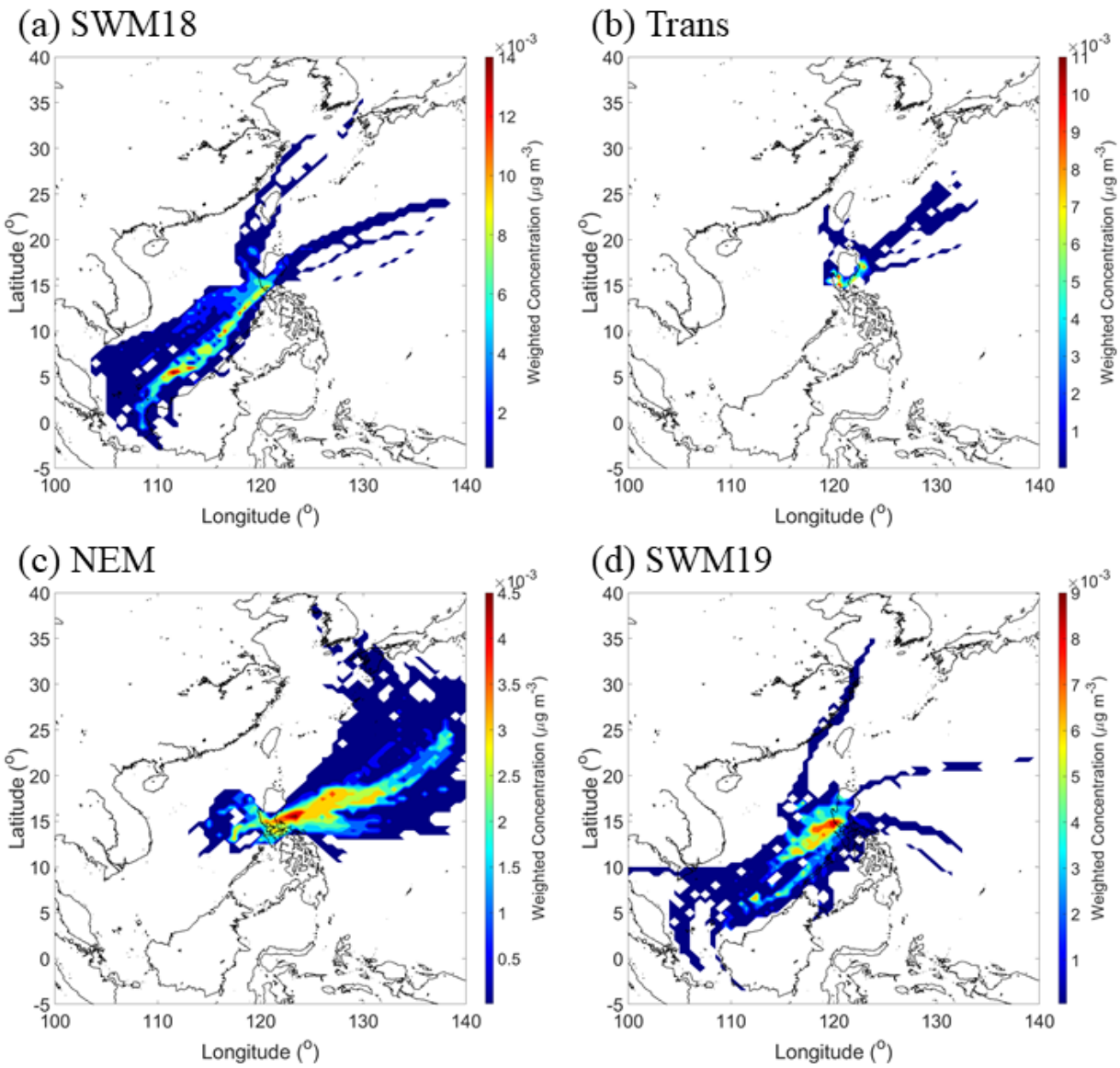

Figure S8: Same as Figure S3 except for MSA.

References

Bardouki, H., Liakakou, H., Economou, C., Sciare, J., Smolík, J., Ždímal, V., Eleftheriadis, K., Lazaridis, M., Dye, C., and Mihalopoulos, N.: Chemical composition of size-resolved atmospheric aerosols in the eastern Mediterranean during summer and winter, Atmos Environ, 37, 195-208, 10.1016/s1352-2310(02)00859-2, 2003.

Blazso, M., Janitsek, S., Gelencsér, A., Artaxo, P., Graham, B., and Andreae, M. O.: Study of tropical organic aerosol by thermally assisted alkylation-gas chromatography mass spectrometry, J Anal Appl Pyrol, 68, 351-369, 10.1016/S0165-2370(03)00082-2, 2003.

Cheng, C., Wang, G., Meng, J., Wang, Q., Cao, J., Li, J., and Wang, J.: Size-resolved airborne particulate oxalic and related secondary organic aerosol species in the urban atmosphere of Chengdu, China, Atmos Res, 161-162, 134-142, 10.1016/j.atmosres.2015.04.010, 2015.

Decesari, S., Fuzzi, S., Facchini, M. C., Mircea, M., Emblico, L., Cavalli, F., Maenhaut, W., Chi, X., Schkolnik, G., Falkovich, A., Rudich, Y., Claeys, M., Pashynska, V., Vas, G., Kourtchev, I., Vermeylen, R., Hoffer, A., Andreae, M. O., Tagliavini, E., Moretti, F., and Artaxo, P.: Characterization of the organic composition of aerosols from Rondônia, Brazil, during the LBA-SMOCC 2002 experiment and its representation through model compounds, Atmos Chem Phys, 6, 375-402, 10.5194/acp-6-375-2006, 2006.

Ding, X. X., Kong, L. D., Du, C. T., Zhanzakova, A., Fu, H. B., Tang, X. F., Wang, L., Yang, X., Chen, J. M., and Cheng, T. T.: Characteristics of size-resolved atmospheric inorganic and carbonaceous aerosols in urban Shanghai, Atmos Environ, 167, 625-641, 10.1016/j.atmosenv.2017.08.043, 2017.

Falkovich, A. H., Graber, E. R., Schkolnik, G., Rudich, Y., Maenhaut, W., and Artaxo, P.: Low molecular weight organic acids in aerosol particles from Rondônia, Brazil, during the biomass-burning, transition and wet periods, Atmos Chem Phys, 5, 781-797, 10.5194/acp-5-781-2005, 2005.

Gao, S., Hegg, D. A., and Jonsson, H.: Aerosol chemistry, and light-scattering and hygroscopicity budgets during outflow from East Asia, J Atmos Chem, 46, 55-88, 10.1023/A:1024821409130, 2003.

Huang, X., Zhang, J., Luo, B., Luo, J., Zhang, W., and Rao, Z.: Characterization of oxalic acid-containing particles in summer and winter seasons in Chengdu, China, Atmos Environ, 198, 133-141, 10.1016/j.atmosenv.2018.10.050, 2019.

Kerminen, V.-M., Teinilä, K., Hillamo, R., and Mäkelä, T.: Size-segregated chemistry of particulate dicarboxylic acids in the Arctic atmosphere, Atmos Environ, 33, 2089-2100, 10.1016/s1352-2310(98)00350-1, 1999.

Maudlin, L. C., Wang, Z., Jonsson, H. H., and Sorooshian, A.: Impact of wildfires on size-resolved aerosol composition at a coastal California site, Atmos Environ, 119, 59-68, 10.1016/j.atmosenv.2015.08.039, 2015.

Mochida, M., Umemoto, N., Kawamura, K., and Uematsu, M.: Bimodal size distribution of C2-C4dicarboxylic acids in the marine aerosols, Geophys Res Lett, 30, 10.1029/2003gl017451, 2003.

Murphy, S. M., Agrawal, H., Sorooshian, A., Padró, L. T., Gates, H., Hersey, S., Welch, W., Jung, H., Miller, J., Cocker III, D. R., Nenes, A., Jonsson, H. H., Flagan, R. C., and Seinfeld, J. H.: Comprehensive simultaneous shipboard and airborne characterization of exhaust from a modern container ship at sea, Environ Sci Technol, 43, 4626-4640, 10.1021/es802413j, 2009.

Neusüss, C., Pelzing, M., Plewka, A., and Herrmann, H.: A new analytical approach for size-resolved speciation of organic compounds in atmospheric aerosol particles: Methods and first results, J Geophys Res-Atmos, 105, 4513-4527, 10.1029/1999jd901038, 2000.

Park, S.-S., and Kim, J.-H.: Possible sources of two size-resolved water-soluble organic carbon fractions at a roadway site during fall season, Atmos Environ, 94, 134-143, 10.1016/j.atmosenv.2014.04.054, 2014.

Sandrini, S., van Pinxteren, D., Giulianelli, L., Herrmann, H., Poulain, L., Facchini, M. C., Gilardoni, S., Rinaldi, M., Paglione, M., Turpin, B. J., Pollini, F., Bucci, S., Zanca, N., and Decesari, S.: Size-resolved aerosol composition at an urban and a rural site in the Po Valley in summertime: implications for secondary aerosol formation, Atmos Chem Phys, 16, 10879-11087, 10.5194/acp-16-10879-2016, 2016.

Sorooshian, A., Csavina, J., Shingler, T., Dey, S., Brechtel, F. J., Saez, A. E., and Betterton, E. A.: Hygroscopic and chemical properties of aerosols collected near a copper smelter: implications for public and environmental health, Environ Sci Technol, 46, 9473-9480, 10.1021/es302275k, 2012.
Turekian, V. C., Macko, S. A., and Keene, W. C.: Concentrations, isotopic compositions, and sources of size-resolved, particulate organic carbon and oxalate in near-surface marine air at Bermuda during spring, J Geophys Res-Atmos, 108, 10.1029/2002JD002053, 2003.
van Pinxteren, D., Neusüß, C., and Herrmann, H.: On the abundance and source contributions of dicarboxylic acids in size-resolved aerosol particles at continental sites in central Europe, Atmos Chem Phys, 14, 3913-3928, 10.5194/acp-14-3913-2014, 2014.
Wang, G., Kawamura, K., Cheng, C., Li, J., Cao, J., Zhang, R., Zhang, T., Liu, S., and Zhao, Z.: Molecular distribution and stable carbon isotopic composition of dicarboxylic acids, ketocarboxylic acids, and alpha-dicarbonyls in size-resolved atmospheric particles from Xi'an City, China, Environ Sci Technol, 46, 4783-4791, 10.1021/es204322c, 2012.
Wang, G., Kawamura, K., Xie, M., Hu, S., Li, J., Zhou, B., Cao, J., and An, Z.: Selected water-soluble organic compounds found in size-resolved aerosols collected from urban, mountain and marine atmospheres over East Asia, Tellus B, 63, 371-381, 10.1111/j.1600-0889.2011.00536.x, 2017.
Yao, X., Fang, M., and Chan, C. K.: Size distributions and formation of dicarboxylic acids in atmospheric particles, Atmos Environ, 36, 2099-2107, 10.1016/s1352-2310(02)00230-3, 2002.
Ziemba, L. D., Griffin, R. J., Whitlow, S., and Talbot, R. W.: Characterization of water-soluble organic aerosol in coastal New England: Implications of variations in size distribution, Atmos Environ, 45, 7319-7329, 10.1016/j.atmosenv.2011.08.022, 2011.